Plasmonics (2023) 18:2195–2204
https://doi.org/10.1007/s11468-023-01938-2

RESEARCH

Optical Biosensor Based on Surface Plasmon Resonance Nanostructure for the Detection of Mycobacterium Tuberculosis Bacteria with Ultra-High Efficiency and Detection Accuracy

Malek G. Daher[1] · Sofyan A. Taya[1] · Abdulkarem H. M. Almawgani[2] · Ayman Taher Hindi[2] · Ilhami Colak[3] · Shobhit K. Patel[4]

Received: 29 May 2023 / Accepted: 3 July 2023 / Published online: 11 July 2023

Abstract

Mycobacterium tuberculosis bacteria is an illness that affects many people worldwide. Early diagnosis is crucial for patient care and can lower the death rate. As a result, sensitive and rapid detection of mycobacterium tuberculosis bacteria in the blood is crucial. In this paper, a novel surface plasmon resonance (SPRE) sensor consisting of a coupling prism, silver (Ag), barium titanate ($BaTiO_3$) and graphene (Gr) layers is presented. The transfer matrix (TM) technique is used for the analysis of the SPRE structure. The Ag and $BaTiO_3$ thicknesses and the number of Gr sheets are optimized to get the highest sensitivity of the proposed SPRE biosensor. The full width at half maximum (FWHM), detection accuracy (DA) and figure of merit (FOM) are investigated. The best performance has been obtained with 65 nm (Ag), and 9 nm ($BaTiO_3$). The number of Gr layers is investigated and optimized to two layers. The highest sensitivity of 300 deg./RIU has been obtained for the proposed SPRE biosensor when the optimized thicknesses are employed. Compared with existing SPRE biosensors in the literature, the proposed sensor exhibits greater sensitivity. The excellent performance makes this SPRE-based sensor promising to be used in numerous biosensing applications.

Keywords Surface plasmon resonance · Mycobacterium tuberculosis · Transfer matrix method · $BaTiO_3$ · Graphene

Introduction

Tuberculosis (TB) is an infectious illness caused by Mycobacterium tuberculosis (MBTS). When a person coughs, for instance, MBTS can spread through the air. TB is a key cause of health worsening and mortality worldwide [1]. TB is a multisystem infectious disease because it affects various organ systems. About 25% of people are thought to have TB due to the high infection rate [2, 3]. The UN set 17 sustainable development goals in 2015, one of which is to eliminate TB by 2030. But TB research is obscured by the resource allocations such as laboratories, manpower, and clinical services [4]. Similar to other infectious illnesses, TB needs early diagnosis since treatment in the early stages can be much more effective. A microscopic examination of sputum smears, a tuberculin test, chest X-ray, tissue biopsy analysis, sputum culture, and computed tomography scan are some of the latest advancements in the diagnosis of tuberculosis. The gold standards for these are bacterial culture and acid-fast bacilli smear microscopy [5]. However, it is predicted that microscopic smear tests can identify pulmonary tuberculosis with a sensitivity of up to 70% [6]. The culture method for detecting TB mycobacterial requires 2–8 weeks and there is a limit to the minimum number of bacteria that can be detected [7]. In comparison to sputum culture, the analysis of sputum after acid-fast (ADF) staining is simpler and faster for the diagnosis of pulmonary TB. ADF staining is fast, inexpensive, and simple. Sample processing, smears thickness, conservation and preparation of the reagents, microscope quality and the proficiency of the

✉ Sofyan A. Taya
staya@iugaza.edu.ps

1 Physics Department, Islamic University of Gaza, P.O. Box 108, Gaza, Palestine

2 Electrical Engineering Department, College of Engineering, Najran University, Najran, Kingdom of Saudi Arabia

3 Department of Electrical and Electronics Engineering, Nisantasi University, Istanbul, Turkey

4 Department of Computer Engineering, Marwadi University, Rajkot-360003, India

technical team can all influence the ADF staining sensitivity and specificity [8]. In order to increase the effectiveness of the currently used techniques, additional investigations have been carried out. For instance, computer-aided tuberculosis detection using digital chest X-ray has become more prevalent in a variety of settings. However, computer-aided detection still requires improvement [9].

A subclass of surface plasmons is the surface plasmons resonance (SPRE). The SPRE sensor is used in a variety of biosensing applications, including the detection, analysis, and characterization of biomolecules and chemicals [10, 11]. Additionally, these detectors are very sensitive and enable real-time analyte measurement [12]. The SPRE sensor exhibits a sharp dip in the resonance profile at the resonance frequency/wavelength at the particular refractive index (RI) of the sensing layer [13]. The most preferred arrangement for the sensor's design is the Kretschmann configuration [14]. In this arrangement, the structure has a prism with a low RI with a metal layer is coated on its surface. The metal layer is responsible for the surface plasmons generation. A 2-dimensional (2D) material is utilized in the SPRE structures to enhance the sensor performance since the metal has low adsorbability [15–18]. To improve the biosensor performance, a Gr sheet can be used. Gr is a planar, 2D honeycomb lattice structure made of carbon atoms. It has exceptional electrical and optical properties [19, 20]. In addition to its outstanding mechanical characteristics, Gr also exhibits electrical conductivity, transparency, and biocompatibility. The strongest material is Gr, which also has a great degree of flexibility. Its tensile strength ranges from 15 to 520 MPa whereas Young's modulus is between 20 and 40 GPa [14]. This makes it the perfect choice for biomedical electronic devices. Additionally, it can accommodate fats, RNA, DNA, and biological tissue. Greater transparency and broadband absorption are characteristics of Gr [21]. Its high surface-to-volume ratio permits the adsorption of biomolecules. The carbon ring-like structure of the biomolecules makes them easily able to interact with the Gr structure. This property increases the biomolecule adsorption in the sensor [22]. An SPRE biosensor using Ag and Gr with a minimum reflectance of 0.4674 and a sensitivity of 176 deg./RIU was proposed [23]. A biosensor using an Ag layer and few layers of Franckeite was proposed with a maximum sensitivity of 188 deg./RIU [24]. A biosensor has been demonstrated which has Au, MoS_2, Ni and Gr and a sensitivity of 229 deg./RIU [25]. An SPRE structure with black phosphorus as a 2D material and Au has been theoretically investigated as a sensor. A sensitivity of 245.5 deg./RIU was achieved [26]. A biosensor consisting of black phosphorus, silicon, and transition metal dichalcogenides (TMDC) has been studied and a sensitivity of 184.6 deg./RIU has been attained [27]. The plasmonic enhancing effects of black phosphorus in an SPRE structure stem from its enhanced light-matter interaction, high carrier mobility, tunable bandgap, and field confinement capabilities. These properties make black phosphorus a promising material for enhancing the sensitivity and performance of SPRE-based biosensors and other plasmonic devices. The effects of TMDC in an SPRE structure arise from their strong light-matter interaction, exciton resonances, tunable optical properties, enhanced energy transfer, and ultrathin nature. These properties make TMDs promising materials for enhancing the sensitivity, selectivity, and overall performance of SPRE-based biosensors. Recent studies show that barium titanate ($BaTiO_3$) possesses unusual dielectric properties such as minimum loss and high RI. Moreover, it is able to create a considerable shift in the resonance SPRE dip with a smaller increment in the RI of an analyte layer [28]. $BaTiO_3$ is a porous material with a 50–70% porosity. The average pore size is about 30 µm in diameter. It was reported that $BaTiO_3$ does not show short-term toxicity [29]. Tetragonal crystalline $BaTiO_3$ nanoparticles display unusual optical properties and biocompatibility. Furthermore, they do not change their morphology [30]. Most of the current SPRE structures suffer the problems of large FWHM, low-quality factor and low sensitivity. Incorporation of a $BaTiO_3$ layer in an SPRE structure offers plasmonic enhancing capabilities through enhanced field localization, tunability of the resonance condition, improved light-matter interaction, and reduced losses. These capabilities contribute to the overall performance and sensitivity of the SPRE sensor [31–33]. Too much work has to be done before SPRE sensors can be commercialized.

In the current paper, a $BaTiO_3$ layer is placed on the top of Ag thin film to improve the biosensor sensitivity, decrease the FWHM of the resonant dip, and improve the quality factor. An additional Gr layer is deposited on the top of the $BaTiO_3$ layer to enhance the adsorption of biomolecules and hence improve the sensor sensitivity to MBTS.

Design Consideration

The He–Ne laser beam with a wavelength of 632.8 nm is coupled into an SPRE nanostructure using a BK7 glass prism with a RI of n_p. The SPRE structure has five layers: BK7 glass prism, Ag, $BaTiO_3$, Gr and analyte medium. The thicknesses of Ag, $BaTiO_3$ and Gr layers are symbolized as $d_{Ag,}$ d_{BaTiO3} and d_G and the RIs are denoted as $n_{Ag,}$ n_{BaTiO3} and n_G, respectively. Figure 1 shows a schematic diagram of the proposed SPRE sensor that is based on $BaTiO_3$-Gr layers.

The BK7 glass prism has a RI given by [34]

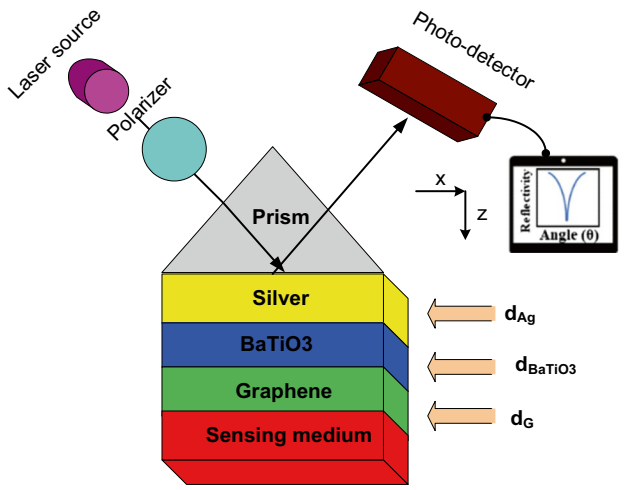

Fig. 1 An SPRE sensor based on $BaTiO_3$- Gr layers

$$n_p(\lambda) = \sqrt{1 + \frac{S_1\lambda^2}{\lambda^2 - U_1} + \frac{S_2\lambda^2}{\lambda^2 - U_2} + \frac{S_3\lambda^2}{\lambda^2 - U_3}} \tag{1}$$

where $S_1 = 1.03961212$, $S_2 = 1.01046945$, $S_3 = 0.231792344$, $U_1 = 0.00600069867$, $U_2 = 103.560653$ and $U_3 = 0.0200179144$.

The RI of the Ag metal is calculated using Drude-Lorentz model [35]

$$n_{Ag}(\lambda) = \left(1 - \frac{\lambda_{cw}\lambda^2}{\lambda_{pw}{}^2\left(\lambda_{cw} + i\lambda\right)}\right)^{1/2} \tag{2}$$

where $\lambda_{cw} = 1.7614 \times 10^{-5} m$ and $\lambda_{pw} = 1.4541 \times 10^{-7} m$ are the collision and plasma wavelengths of Ag. The RI of Gr can be calculated as [36]

$$n_G(\lambda) = 3 + \lambda\frac{\varphi}{3}i, \varphi = 5.446\mu\text{m}^{-1} \tag{3}$$

The RI of $BaTiO_3$ is 2.0 at λ = 632.8 nm [35].

Only p-polarized light (TM-polarization) in naturally occurring materials with positive permittivity and permeability exhibits the phenomenon of SPRE. The angular modulation method can be used to study the proposed structure. With the use of the TM technique and Fresnel theory, the reflectance of waves (p-polarized) can be studied. For the surface plasmon to be stimulated, the propagation constants of the wave and the surface plasmon must be equal. In a mathematical form

$$\frac{\omega}{c}\sqrt{\varepsilon_p}sin\theta_i = \frac{\omega}{c}\sqrt{\frac{\varepsilon_{Ag}\varepsilon_d}{\varepsilon_{Ag}+\varepsilon_d}} \tag{4}$$

where ε_p, ω, ε_{Ag}, θ_i and ε_d are the dielectric permittivity of the prism, the incident radiation frequency, the metal dielectric permittivity, the incident angle and the dielectric permittivity, respectively.

Along the z-axis, several layers are stacked. The tangential field components at the first interface can be written in terms of those at the last interface as

$$\begin{bmatrix} X_1 \\ H_1 \end{bmatrix} = B_T \begin{bmatrix} X_{N-1} \\ H_{N-1} \end{bmatrix} \tag{5}$$

where X_1 (H_1) and $X_{N\text{-}1}$ ($H_{\text{N-1}}$) are the tangential electric (magnetic) fields at the first and the last boundaries, respectively. B_T is the TM that relates the field components to these boundaries. For the j[th] layer, the TM (B_j) can be written as

$$B_j = \begin{bmatrix} \cos(U_j) & -\frac{i\sin(U_j)}{P_j} \\ -iP_j\sin(U_j) & \cos(U_j) \end{bmatrix} \tag{6}$$

U_j is the phase shift which is given by

$$U_j = \frac{2\pi}{\lambda}d_j\left(\varepsilon_j - (n_1\sin\theta_1)^2\right)^{0.5} \tag{7}$$

where n_1 and θ_1 are the RI and the incident angle of the prism.

For TM waves, P_j is defined as

$$P_j = \left(\varepsilon_j - (n_1\sin\theta_1)^2\right)^{0.5}/\varepsilon_j \tag{8}$$

The system TM (B_T) of the structure can be written as

$$B_T = B_{Ag}B_{BaTiO3}B_G = \begin{bmatrix} B_{11} & B_{12} \\ B_{21} & B_{22} \end{bmatrix} \tag{9}$$

where B_{Ag}, B_{BaTiO3} and B_G are the TMs of the Ag, $BaTiO_3$ and Gr layers.

The reflection coefficient (r) of the structure is given in terms of B_{ij} as

$$r = \frac{\left(B_{11} + B_{12}P_N\right)P_1 - \left(B_{21} + B_{22}P_N\right)}{\left(B_{11} + B_{12}P_N\right)P_1 + \left(B_{21} + B_{22}P_N\right)} \tag{10}$$

The reflectivity (R) of the proposed SPRE nanostructure is given by

$$R = r.r^* = |r|^2 \tag{11}$$

Sensitivity (S), FWHM, detection accuracy (DA), and figure of merit (FOM) of SPRE sensors are usually estimated for the sensor performance. When a change in the RI (Δn) of the sensing medium occurs, the resonant angle shifts by an amount $\Delta\theta_{res}$. The sensitivity depends on both Δn and $\Delta\theta_{res}$ according to

$$S = \frac{\Delta\theta_{res}}{\Delta\text{n}} \tag{12}$$

The FWHM is obtained from the reflectance curve as

$$FWHM = \theta_2 - \theta_1 \tag{13}$$

where θ_1 and θ_2 are the resonance angles at 50% reflectivity.

DA is the reciprocal of the FWHM multiplied by $\Delta\theta_{res}$.

$$DA = \frac{\Delta\theta_{res}}{FWHM} \tag{14}$$

FOM is the product of S and DA of the sensor

$$FOM = S \times DA \tag{15}$$

The quality factor (QF) of an SPRE can be calculated as

$$QF = \frac{\mathrm{S}}{FWHM} \tag{16}$$

Results and Discussion

Fabrication Feasibility

This subsection describes the steps involved in fabricating the proposed multilayer SPRE chip. Initially, a solution containing acetone, methanol, and deionized water is applied to the BK7 prism. Subsequently, a thin silver film is coated onto the prism using a deposition technique such as thermal evaporation or physical vapor deposition. To synthesize the $BaTiO_3$ material, a hydrothermal reaction is carried out by reacting TiO_2 with an aqueous solution of $Ba(OH)_2$. This reaction results in the formation of highly crystallized and well-dispersed perovskite-type $BaTiO_3$. For the production of a single layer of graphene, chemical vapor deposition is considered the most promising method as it yields high-quality single-layer graphene. Subsequently, a blood sample is poured onto the sensor chip area for sensing purposes. The entire SPRE chip is then placed on a rotating table, and an optical detector positioned at the output side of the prism receives the reflected light and determines its intensity.

MBTS Sensor

An SPRE structure-based optical sensor is investigated for sensing MBTS bacteria. The following calculations will be conducted at $\lambda = 632.8$ nm. The SPRE sensor has five layers: BK7 glass prism, Ag, $BaTiO_3$, Gr and analyte medium. The RIs of "Design Consideration" to the expressions presented in Sect. 2. The RIs of the materials are given by $n_p = 1.5151$, $n_{Ag} = 0.056206 + 4.2776i$, $n_{BaTiO3} = 2$ and $n_G = 3 + 1.1487i$ for BK7 glass prism, Ag, $BaTiO_3$ and Gr. Layer thicknesses are initially chosen as $d_{Ag} = 40$ nm, $d_{BaTiO3} = 1$ nm and $d_G = L \times 0.34$ nm where L is the number of Gr layers (initially, L = 1). Either a normal blood sample (NBSE) or a sample infected with tuberculosis bacteria (TBj), j = 1—4 makes up the analyte layer. The RIs of NBSE and TBj samples are reported in Table 1 [37]. We have used Wolfram Mathematica 11.2 software to conduct the simulation. Figure 2 shows the reflectance curves when NBSE and TBi are handled as sensing media. The figure shows a resonant dip at a resonant angle of 71.19 deg. when NBSE is used as a sensing medium. When TBi samples are used as sensing media, the resonant angle moves to a lower angle region. The dip angular position is found cell-dependent. They are at 70.79, 70.66, 70.41 and 70.16 deg. for TB1, TB2, TB3 and TB4 cells. The sensitivity is found as 133.33, 132.5, 130 and 128.75 deg./RIU for TB1, TB2, TB3 and TB4 cells. Table 1 displays the RIs of different samples, the dip position, and the sensitivity of the proposed SPRE biosensor to each cell.

Table 1 Dip position and sensitivity to tuberculosis cells. ($d_{Ag} = 40$ nm, $d_{BaTiO3} = 1$ nm, and $d_G = 1 \times 0.34$ nm)

Sensing medium	RI	Dip Angle (deg.)	Angular shift (deg.)	S (deg./RIU)
NBSE	1.351	71.19	-	-
TB1	1.348	70.79	0.4	133.33
TB2	1.347	70.66	0.53	132.5
TB3	1.345	70.41	0.78	130
TB4	1.343	70.16	1.03	128.75

Effect of Ag Layer Thickness

A proper selection of the layer thicknesses of the SPRE structure is necessary and can significantly enhance the sensor performance. This subsection and the following include an investigation of the various options for layer thicknesses. So, for a constant thickness of $BaTiO_3$ ($d_{BaTiO3} = 1$ nm) and

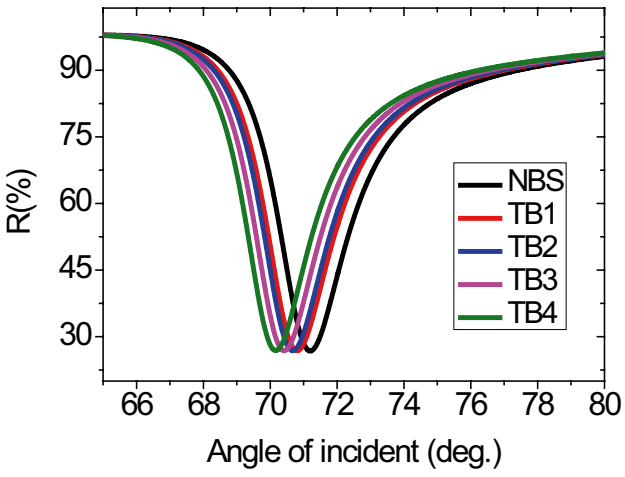

Fig. 2 Reflectivity versus the θ_i at $d_{Ag} = 40$ nm, $d_{BaTiO3} = 1$ nm, and $d_G = 1 \times 0.34$ nm

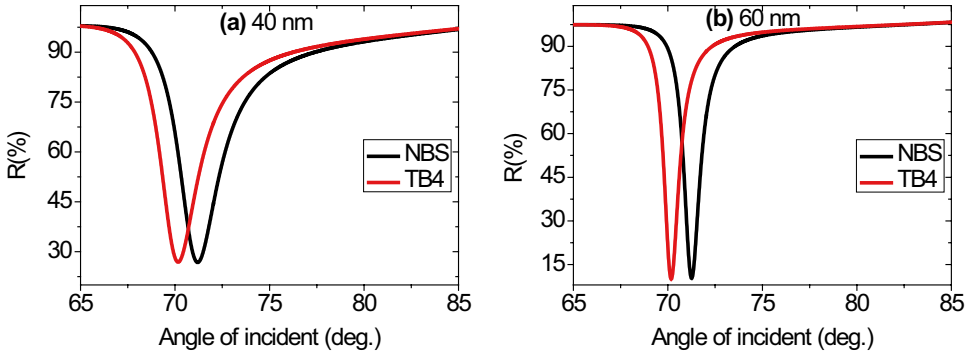

Fig. 3 Reflectivity versus the incidence angle at $d_{BaTiO3} = 1$ nm, and $d_G = 1 \times 0.34$ nm. **a** $d_{Ag} = 40$ nm and **b** $d_{Ag} = 60$ nm

a monolayer of Gr (L = 1), we study the effect of the Ag thickness on the SPRE sensor performance. We consider two samples here: NBSE and TB4. The Ag thickness is varied from 40 – 65 nm in a step of 5 nm. The reflectance spectrum corresponding to each Ag thickness is studied and some of these spectra are illustrated in Fig. 3(a) and (b) for $d_{Ag} = 40$ nm and 60 nm, respectively. Figure 4 illustrates the sensitivity variation for different thicknesses for the Ag layer which shows an increase from 128.75 deg./RIU at $d_{Ag} = 40$ nm to 136.25 deg./RIU at $d_{Ag} = 65$ nm. The sensitivity shows a maximum at $d_{Ag} = 65$ nm. Table 2 reports the variation of the dip angular position, angular shift and sensitivity corresponding to different Ag layer thicknesses. Table 3 presents the variation of FWHM, DA, and FOM for different thicknesses of Ag. The FWHM decreases from 2.35 to 0.82 deg. as the Ag thickness increases from 40 to 65 nm. This decrease in the FWHM significantly improves the DA of the SPRE sensor, as shown in Table 3. It is obvious that when the Ag layer thickness increases, the DA rises as well. The maximum DA is 1.219512195 deg.$^{-1}$ at $d_{Ag} = 65$ nm. The FOM also enhances as the Ag thickness rises because both the sensitivity and the DA are enhanced.

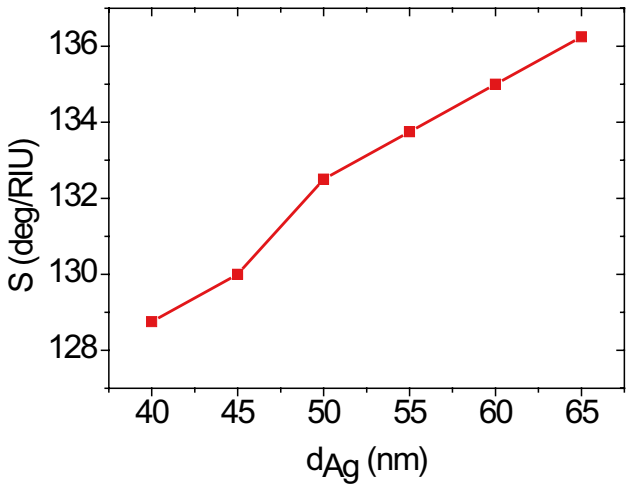

Fig. 4 S versus d_{Ag} at $d_{BaTiO3} = 1$ nm and a monolayer of Gr

Table 2 Variation of the angular position and sensitivity for different Ag thicknesses at $d_{BaTiO3} = 1$ nm and a monolayer of Gr

Ag thickness (nm)	Dip of NBSE (deg.)	Dip of TB4 (deg.)	Angular shift (deg.)	S (deg./RIU)
40	71.19	70.16	1.03	128.75
45	71.21	70.17	1.04	130
50	71.23	70.17	1.06	132.5
55	71.25	70.18	1.07	133.75
60	71.26	70.18	1.08	135
65	71.28	70.19	1.09	136.25

As the thickness of the Ag layer increases, the transfer of incident wave energy to surface plasmon is dramatically enhanced. This causes an efficient excitation of surface plasmon which leads to a very high sensitivity and quality of the SPRE sensor. Consequently, the optimized Ag layer thickness is 65 nm which corresponds to the best performance. It is worth mentioning that if the Ag layer thickness is increased above 65 nm, the resonance dip disappears. So, a thickness of 65 nm can be considered as optimum.

Effect of $BaTiO_3$ Layer Thickness

The thickness of $BaTiO_3$ layer is varied in the range from 1 – 9 nm and the reflectance spectrum is studied for each

Table 3 Variation of the sensor performance parameters for different thicknesses of Ag at $d_{BaTiO3} = 1$ nm and a monolayer of Gr

Ag thickness (nm)	FWHM (deg.)	DA	FOM (deg./RIU)	QF (1/RIU)
40	2.35	0.438297872	56.430	54.787
45	1.92	0.541666667	70.416	67.708
50	1.44	0.736111111	97.534	92.013
55	1.21	0.884297521	118.274	110.537
60	1.02	1.058823529	142.941	132.352
65	0.82	0.438297872	181.112	166.158

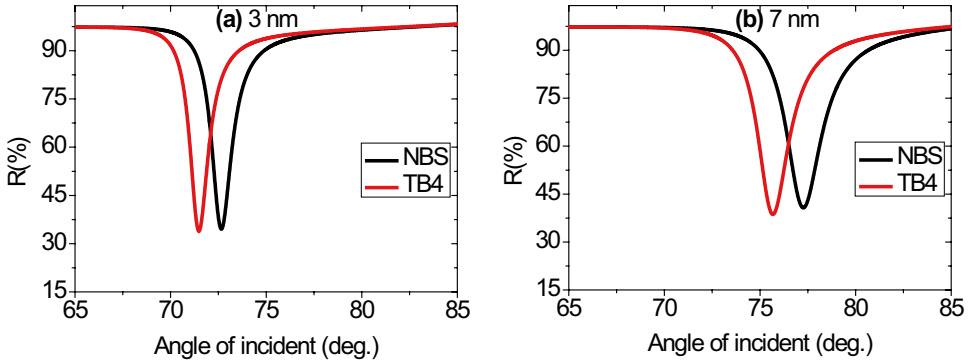

Fig. 5 Reflectivity versus the incidence angle at $d_{Ag}=65$ nm, and $d_G=1\times0.34$ nm. **a** $d_{BaTiO3}=3$ nm and **b** $d_{BaTiO3}=7$ nm

thickness. Two of these spectra are shown in Fig. 5 for the normal blood and TB4 samples. The sensitivity is observed to enhance with the increase of $BaTiO_3$ layer thickness (Fig. 6). It increases from 136.25 to 267.5 deg./RIU as the thickness of $BaTiO_3$ increases from 1 to 9 nm as reported in Table 4. The sensitivity is considerably improved by 96.33% due to the increase in the $BaTiO_3$ layer thickness. The angular position of the resonant dip shifts to higher angles as the thickness of $BaTiO_3$ increases. On the other hand, inspection of Table 5 shows that the FWHM of the SPRE dips gets broader and broader as d_{BaTiO3} thickness increases from 1 to 9 nm which indicates that the energy loss of the SPRE biosensor is gradually enhanced with increasing the thickness of $BaTiO_3$ layer. Since DA is the reciprocal of FWHM, it is reduced as d_{BaTiO3} increases as presented in Table 5. When d_{BaTiO3} changes from 1 to 9 nm, the DA decreases from 1.219512195 to 0.418410042 $deg.^{-1}$ which means a decline by about 65.7% of its initial value. Moreover, Table 5 pointed out that a gradual decrease has occurred in FOM owing to the increase of $BaTiO_3$ layer thickness. It is observed that the resonant dip disappears for $d_{BaTiO3}>9$ nm.

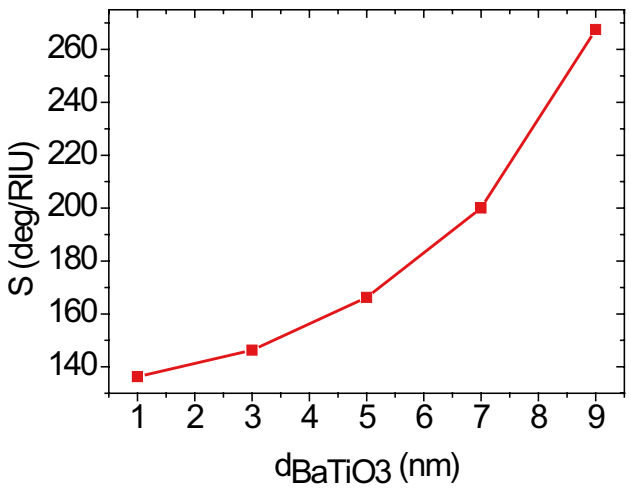

Fig. 6 S versus d_{BaTiO3} at $d_{Ag}=65$ nm and a monolayer of Gr

Table 4 Variation of the angular position and sensitivity for different $BaTiO_3$ thicknesses at $d_{Ag}=65$ nm and a monolayer of Gr

$BaTiO_3$ thickness (nm)	Dip of NBSE (deg.)	Dip of TB4 (deg.)	Angular shift (deg.)	S (deg./RIU)
1	71.28	70.19	1.09	136.25
3	72.66	71.49	1.17	146.25
5	74.66	73.33	1.33	166.25
7	77.28	75.68	1.6	200
9	81	78.86	2.14	267.5

Effect of the Number of Gr Layers

The sensor performance is examined as the number of Gr layers varies. The Ag and $BaTiO_3$ are kept constant at 65 nm and 9 nm, respectively. Figures 7(a) and (b) show some of the spectra for Gr layers with L = 1 and L = 3, respectively. The sensitivity rises as the number of Gr sheets increases from L = 1 to L = 2 (Fig. 8). A further increase in the number of Gr sheets above L = 2 leads to a sensitivity decline as shown in Table 6. The greater absorption due to the imaginary part of the Gr dielectric constant is responsible for the sensitivity decline as more sheets of Gr are added [38, 39]. However, in a similar manner to increasing the $BaTiO_3$ layer thickness, any growth of the number of Gr sheets above L = 1 is accompanied by

Table 5 Variation of the sensor performance parameters for different thicknesses of $BaTiO_3$ at $d_{Ag}=65$ nm and a monolayer of Gr

$BaTiO_3$ Thickness (nm)	FWHM (deg.)	DA	FOM (deg./RIU)	QF (1/RIU)
1	0.82	1.329268293	181.112	166.158
3	1.22	0.959016393	140.256	119.877
5	1.43	0.93006993	154.624	116.258
7	1.73	0.924855491	184.971	115.606
9	2.39	0.89539749	239.518	111.924

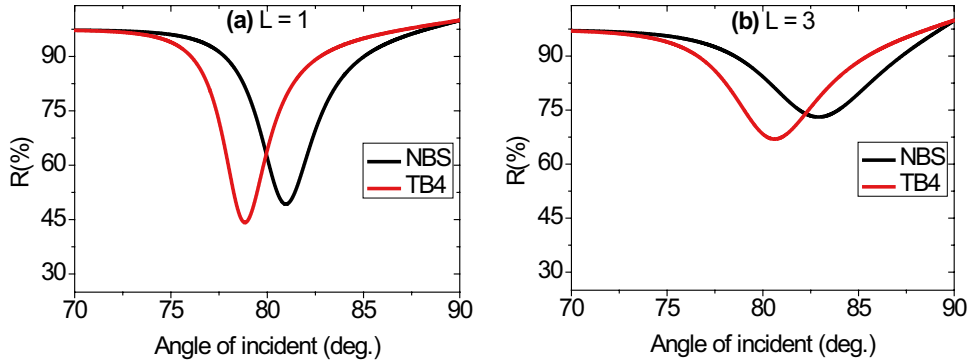

Fig. 7 Reflectivity versus θ_i at $d_{Ag}=65$ nm, and $d_{BaTiO3}=9$ nm. $d_G=L\times 0.34$ nm where **a** $L=1$ and **b** $L=3$

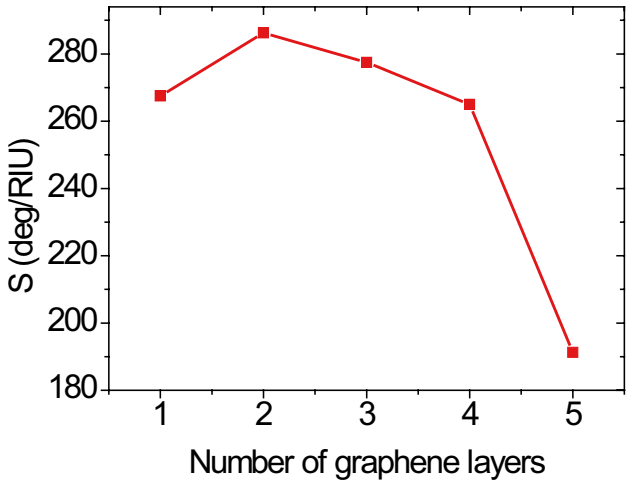

Fig. 8 S versus L (number of Gr sheets) at $d_{Ag}=65$ nm, and $d_{BaTiO3}=9$ nm

Table 6 Variation of the angular position and sensitivity for different numbers of Gr layers at $d_{Ag}=65$ nm and $d_{BaTiO3}=9$ nm

Gr sheets	Dip of NBSE (deg.)	Dip of TB4 (deg.)	Angular shift (deg.)	S (deg./RIU)
1	81	78.86	2.14	267.5
2	81.98	79.69	2.29	286.25
3	82.84	80.62	2.22	277.5
4	83.59	81.47	2.12	265
5	83.7	82.17	1.53	191.25

Table 7 Variation of FWHM, DA, and FOM for different numbers of Gr layers at $d_{Ag}=65$ nm and $d_{BaTiO3}=9$ nm

Number of Gr layers	FWHM (deg.)	DA	FOM (deg./RIU)	QF (1/RIU)
1	2.39	0.89539749	239.518	111.924
2	3.05	0.750819672	214.922	93.852
3	4.29	0.517482517	143.601	64.685
4	5.42	0.391143911	103.653	48.892
5	5.91	0.258883249	49.511	32.360

a FWHM enhancement which has a negative impact on the DA and FOM of the proposed sensor (Table 7). The FWHM is directly proportional to damping in the surface plasmons which enhances with an increase in the number of Gr sheets due to the imaginary part of the Gr dielectric constant [40]. Therefore, it can be inferred that the performance of the SPRE sensor will deteriorate as the number of Gr sheets increases. A Gr bilayer may be the best choice for the proposed SPRE biosensor.

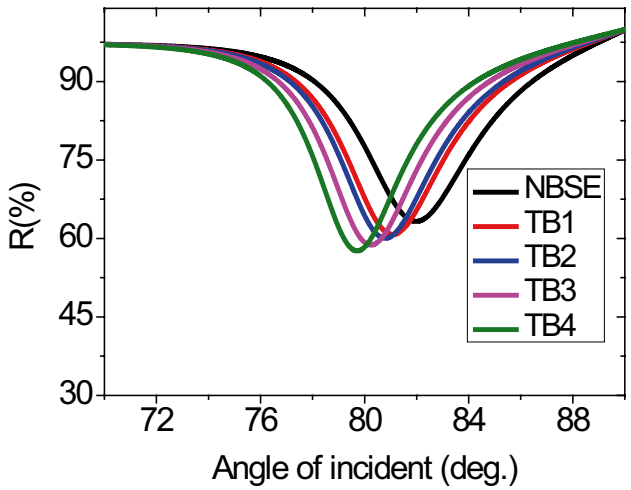

Fig. 9 Reflectivity versus the incidence angle at $d_{Ag}=65$ nm, $d_{BaTiO3}=9$ nm, and $d_G=2\times 0.34$ nm

Table 8 Dip angular position and sensitivity to different tuberculosis cells at $d_{Ag}=65$ nm, $d_{BaTiO3}=9$ nm, and $d_G=2\times 0.34$ nm

Sensing medium	RI	Dip position (deg.)	Angular shift (deg.)	S (deg./RIU)
NBSE	1.351	81.98	-	-
TB1	1.348	81.08	0.9	300
TB2	1.347	80.79	1.19	297.5
TB3	1.345	80.24	1.74	290
TB4	1.343	79.69	2.29	286.25

Table 9 Variation of FWHM, DA, and FOM of different samples of TB bacteria at the optimized parameters

Sensing medium	RI	FWHM (deg.)	DA	FOM (deg./RIU)	QF (1/RIU)
NBSE	1.351	4.15	-	-	-
TB1	1.348	3.61	0.249307479	74.792	83.102
TB2	1.347	3.46	0.343930636	102.319	85.982
TB3	1.345	3.37	0.516320475	149.732	86.053
TB4	1.343	3.05	0.68358209	195.675	85.447

Table 10 Comparing the sensitivity of the current work with the most recent works

Structure	Analyte	S (deg/RIU)	QF (1/RIU)	DA	FOM (deg./RIU)	Ref
SPRE sensor employing three sheets of Gr	Any sensing medium	121.67	36.87	2.21	-	[41]
SPRE sensor for DNA hybridization utilizing a ZnO layer	DNA hybridization	156.33	-	0.64	9.14	[42]
SPRE sensor consisting of prism/ ZnO/ Au/ Blue phosphorus-MoS_2/ Sensing medium	Any sensing medium	235	56.211	0.281	-	[43]
SPRE sensor based on black phosphorus 2D material	Blood plasma	124	19.94	0.159	-	[44]
Gr sheets-based SPRE biosensor	Any sensing medium	103	-	-	-	[45]
Detection of TB using SPRE modulated by telecommunication wavelength	TB	0.087 dB/(μg/mL)	-	-	-	[46]
SPRE based fiber for TB detection	TB	5000 nm/RIU	-	-	-	[47]
SPRE sensor based on $BaTiO_3$-Gr layers	TB	300	83.102	0.249	74.792	our work

Tuberculosis Sensor Optimization

The optimal conditions are $d_{Ag} = 65$ nm, $d_{BaTiO3} = 9$ nm, and $d_G = L \times 0.34$ nm where $L = 2$. At these conditions, the reflectance is investigated in Fig. 9 for all samples which displays that the angular dip shifts to lower angles of incidence as the tuberculosis-infected samples replace the NBSE. The angular positions of the resonant dips along with sensitivity are reported in Table 8. The sensitivity of the optimized SPRE structure is found as 300, 297.5, 290 and 286.25 deg./RIU for the samples of TB1, TB2, TB3 and TB4. Additionally, Table 9 displays the FWHM, DA, and FOM which are all indicators of the sensor performance. Based on these values, the proposed $BaTiO_3$-Gr-based SPRE sensor exhibits good performance with the optimum layer thicknesses. Table 10 also offers a comparison of the current and previously reported works. With this performance, we believe that the proposed $BaTiO_3$-Gr-based SPRE sensor can find widespread use in the field of biosensing technologies.

Conclusion

An SPRE-based biosensor based on $BaTiO_3$-Gr layers has been theoretically suggested and numerically investigated for sensing tuberculosis bacteria in the blood. The reflectivity of TM-polarized waves using the TM technique has been analyzed. Silver (Ag), barium titanate ($BaTiO_3$), and Gr thicknesses of the proposed SPRE sensor have been optimized. When the thicknesses are taken as $d_{Ag} = 40$ nm, $d_{BaTiO3} = 1$ nm and $d_G = L \times 0.34$ nm ($L = 1$), a sensitivity of about 130 deg./RIU has been obtained. When the Ag layer thickness increases, all the sensor performance parameters are enhanced. This can be attributed to the following: as the Ag thickness increases, the transfer of incident light energy to surface plasmon is dramatically enhanced. This leads to an efficient excitation of surface plasmon. When the $BaTiO_3$ thickness is increased, the sensitivity is observed to considerably improved by 96.33%. On the other hand, the FWHM of the SPRE dips gets broader and broader as d_{BaTiO3} thickness increases which indicates that the energy loss of the SPRE biosensor is gradually enhanced with increasing the thickness of $BaTiO_3$ layer. When the number of Gr layers increases, the sensitivity rises as the layers of Gr sheets increase from $L = 1$ to $L = 2$. A further increase in the number of Gr sheets above $L = 2$ leads to a sensitivity decline. The optimal conditions of the SPRE structure are found as $d_{Ag} = 65$ nm, $d_{BaTiO3} = 9$ nm, and $d_G = L \times 0.34$ nm where $L = 2$ at which the sensitivity can reach about 300 deg./RIU. It is believed the proposed $BaTiO_3$-Gr-based SPRE sensor can find widespread use in the field of biosensing technologies.

Acknowledgements The authors are thankful to the Deanship of Scientific Research at Najran University for funding this work under the Research Groups Funding program grant code (NU/RG/SERC/12/4).

Author Contribution The authors confirm their contribution to the paper as follows: study conception and design (Sofyan A. Taya and Malek G. Daher). Software (Abdulkarem H. M. Almawgani). Interpretation of results (Malek G. Daher and Ilhami Colak). Draft manuscript preparation (Ayman Taher Hindi and Malek G. Daher). Writing the final version (Shobhit K. Patel and Sofyan). Supervision (Sofyan A. Taya). All authors reviewed the results and approved the final version of the manuscript.

Funding Deanship of Scientific Research at Najran University.

Availability of Data and Material Detail about data has been provided in the article.

Code Availability The used code can be obtained from the corresponding author upon request.

Declarations

Ethics Approval This study does not require ethics approval.

Consent to Participate No consent to participate is required for this study.

Consent for Publication No consent for publication is required for this study.

Conflicts of Interest The authors declare no conflict of interest.

References

1. World Health Organization (2022) Global Tuberculosis Report 2022. WHO, Geneva, Switzerland
2. Houben RMGJ, Dodd PJ (2016) The Global Burden of Latent Tuberculosis Infection: A Re-estimation Using Mathematical Modelling. PLoS Med 13:e1002152
3. Hrizi O, Gasmi K, Ben Ltaifa I, Alshammari H, Karamti H, Krichen M, Ben Ammar L, Mahmood MA (2022) Tuberculosis Disease Diagnosis Based on an Optimized Machine Learning Model. J Healthc Eng 8950243
4. Sahu S, Wandwalo E, Arinaminpathy N (2022) Exploring the Impact of the COVID-19 Pandemic on Tuberculosis Care and Prevention. J Pediatric Infect Dis Soc 11:S67–S71
5. Wang CH, Chang JR, Hung SC, Dou HY, Lee GB (2022) Rapid molecular diagnosis of live Mycobacterium tuberculosis on an integrated microfluidic system. Sensor Actuat B-Chem 365:131968
6. Azadi D, Motallebirad T, Ghaffari K, Shojaei H (2018) Mycobacteriosis and Tuberculosis: Laboratory Diagnosis. Open Microbiol J 12:41–58
7. Soini H, Musser JM (2001) Molecular diagnosis of mycobacteria. Clin Chem 47:809–814
8. Vilcheze C, Kremer L (2017) Acid-Fast Positive and Acid-Fast Negative Mycobacterium tuberculosis: The Koch Paradox. Microbiol Spectr 5:1–14
9. Pande T, Cohen C, Pai M, Khan FA (2016) Computer-aided detection of pulmonary tuberculosis on digital chest radiographs: A systematic review. Int J Tuberc Lung D 20:1226–1230
10. Mustafa F, Andreescu S (2018) Chemical and biological sensors for food-quality monitoring and smart packaging. J Food Sci Technol 49(4):383–406
11. Bhatia S, Jiang YC, Sun MJ, Xiong RJ (2018) Development of a surface plasmon resonance acetone sensor for noninvasive screening and monitoring of diabetes. Mater Sci Eng 383:012024
12. Srivastava A, Prajapati YK (2019) Performance Analysis of Silicon and Blue Phosphorene / MoS 2 Hetero-Structure Based SPRE Sensor. Photonic Sens 9(3):284–292
13. De Melo AA, Brito T, Fernanda M, Moreira S, Moreno R, Cruz S (2018) Theoretical analysis of sensitivity enhancement by graphene usage in optical Fiber surface plasmon resonance sensors. IEEE Trans Instrum Meas 68(5):1554–1560
14. Pal A, Jha A (2021) A theoretical analysis on sensitivity improvement of an SPRE refractive index sensor with graphene and barium titanate nanosheets. Optik - International Journal for Light and Electron Optics 231:166378
15. Bhardwaj S, Pathak NK, Ji A et al (2017) Tunable Properties of Surface Plasmon Resonance of Metal Nanospheroid: Graphene Plasmon Interaction. Plasmonics 12:193–201. https://doi.org/10.1007/s11468-016-0249-7
16. Arsalani S, Ghodselahi T, Neishaboorynejad T et al (2019) DNA Detection Based on Localized Surface Plasmon Resonance Spectroscopy of Ag@Au Biocomposite Nanoparticles. Plasmonics 14:1419–1426. https://doi.org/10.1007/s11468-019-00937-6
17. Alaguvibisha G et al (2020) Sensitivity enhancement of surface plasmon resonance sensor using hybrid configuration of 2D materials over bimetallic layer of Cu-Ni. Opt Commun 463:125337
18. Vahedi A, Kouhi M (2020) Liquid crystal-based surface plasmon BiosensorResonance. Plasmonics 15:61–71
19. Song B, Li D, Qi W, Elstner M, Fan C, Fang H (2010) Graphene on Au (111): A Highly Conductive Material with Excellent Adsorption Properties for High-Resolution Bio / Nanodetection and Identification. ChemPhysChem 19(111):585–589
20. Papageorgiou DG, Kinloch IA, Young RJ (2017) Progress in Materials Science Mechanical properties of graphene and graphene-based nanocomposites. Prog Mater Sci 90:75–127
21. Reina G, Gonz´alez-Domínguez JM, Criado A, V´azquez E, Bianco A, Prato M (2017) Promises, facts and challenges for graphene in biomedical applications. Chem Soc Rev 46(15):4400–4416
22. Aksimsek S, Jussila H, Sun Z (2018) Graphene – MoS 2 – metal hybrid structures for plasmonic biosensors. Opt Commun 428:233–236
23. Dai X, Liang Y, Zhao Y, Gan S, Jia Y, Xiang Y (2019) Sensitivity enhancement of a surface plasmon resonance with tin selenide (SnSe) allotropes. Sensors 19(1):173
24. Gan S, Zhao Y, Dai X, Xiang Y (2019) Sensitivity enhancement of surface plasmon resonance sensors with 2D franckeite nanosheets. Results Phys 13:102320
25. Nisha A, Maheswari P, Anbarasan PM, Rajesh KB, Jaroszewicz Z (2019) Sensitivity enhancement of surface plasmon resonance sensor with 2D material covered noble and magnetic material (Ni). Opt Quantum Electron 51(1)
26. Singh Y, Raghuwanshi SK (2019) Electromagnetic wave sensors sensitivity enhancement of the surface plasmon resonance gas sensor with black phosphorus. IEEE Sensors Lett 3(12):1–4
27. Pal S, Verma A, Saini JP, Prajapati YK (2019) Sensitivity enhancement using silicon-black phosphorus-TDMC coated surface plasmon resonance biosensor. IET Optoelectron 13(4):196–201
28. Singh Y, Paswan MK, Raghuwanshi SK (2020) Sensitivity enhancement of SPRE sensor with the black phosphorus and graphene with Bi-layer of gold for chemical sensing. Plasmonics
29. Ball JP, Mound BA, Nino JC, Allen JB (2014) Biocompatible evaluation of barium titanate foamed ceramic structures for orthopedic applications. J Biomed Mater Res - Part A 102(7):2089–2095
30. Marino A et al (2019) Piezoelectric barium titanate nanostimulators for the treatment of glioblastoma multiforme. J Colloid Interface Sci 538:449–461

31. Mudgal N, Saharia A, Choure KK et al (2020) Sensitivity enhancement with anti-reflection coating of silicon nitride (Si3N4) layer in silver-based Surface Plasmon Resonance (SPR) sensor for sensing of DNA hybridization. Appl Phys A 126:946. https://doi.org/10.1007/s00339-020-04126-9
32. Mudgal N, Yupapin P, Ali J et al (2020) BaTiO3-Graphene-Affinity Layer-Based Surface Plasmon Resonance (SPR) Biosensor for Pseudomonas Bacterial Detection. Plasmonics 15:1221–1229. https://doi.org/10.1007/s11468-020-01146-2
33. Wang S, Zhang J, Liu N et al (2023) Sensitivity Improvement of Bimetallic Layer-Based SPR Biosensor Using ZnO and Black Phosphorus. Plasmonics. https://doi.org/10.1007/s11468-023-01889-8
34. Lin Z, Jiang L, Wu L, Guo J, Dai X, Xiang Y, Fan D (2016) Tuning and sensitivity enhancement of surface plasmon resonance biosensor with graphene covered Au MoS2-Au films. IEEE Photon J 8(6):1–8
35. Sun P, Wang M, Liu L, Jiao L, Wei Du, Xia F, Liu M, Kong W, Dong L, Yun M (2019) Sensitivity enhancement of surface plasmon resonance biosensor based on graphene and barium titanate layers. Appl Surf Sci 475:342–347
36. Bruna M, Borini S (2009) Optical constants of graphene layers in the visible range. Appl Phys Lett 94(3):03190
37. Reddy NM, Kothandan D, Lingam SC, Ahmad A (2012) A study on refractive index of plasma of blood of patients suffering from tuberculosis. Int J Technol Eng 8:23–25
38. Lin C, Chen S (2019) Design of high-performance Au-Ag-dielectric-graphene based surface plasmon resonance biosensors using genetic algorithm. J Appl Phys 125:113101
39. Lin C, Chen S (2019) Sensitivity comparison of graphene based nearly guided-wave surface plasmon resonance biosensors with Au, Ag, Cu, and Al. J Nanophotonics 13:016006
40. Maharana PK, Jha R (2012) Chalcogenide prism and graphene multilayer based surface plasmon resonance affinity biosensor for high performance. Sens Actuat B Chem 169:161–166
41. Hossain MB, Mehedi IM, Moznuzzaman M, Abdulrazak LF, Hossain MA (2019) High performance refractive index SPRE sensor modeling employing graphene tri sheets, Vol. 15, Results in Physics, p. 102719
42. Pal S, Prajapati YK, Saini JP (2020) Influence of grapheme'chemical potential on SPRE biosensor using ZnO for DNA hybridization, Vol. 27, Optical Review, pp. 57–64
43. Singh S, Sharma AK, Lohia P, Dwivedi DK (2021) Theoritical analysis of sensitivity enhancement of surface plasmon resonance biosensor with zinc oxide and blue phosphorus/MoS2 heterostructure, Vol. 244, Optik, p. 167618
44. Almawgani AHM, Daher MG, Taya SA, Olaimat MM, Alhawari ARH, Colak I (2022) Detection of blood plasma concentration theoretically using SPR-based biosensor employing black phosphor layers and different metals. Plasmonics 17(4):1751–1764
45. Taya SA, Al-Ashi NE, Ramahi OM, Colak I, Amiri IS (2021) Surface plasmon resonance-based optical sensor using a thin layer of plasma. J Opt Soc Am B 38(8):2362–2367. https://doi.org/10.1364/JOSAB.420129
46. Hsu SH, Lin YY, Lu SH, Tsai IF, Lu YT, Ho HT (2013) Mycobacterium tuberculosis DNA detection using surface plasmon resonance modulated by telecommunication wavelength. Sensors (Basel) 14(1):458–467. https://doi.org/10.3390/s140100458. PMID: 24379050; PMCID: PMC3926568
47. Kaur B, Kumar S, Kaushik BK (2022) Antimonene, CNT and MoS2 Based SPR-Fiber-Optic Probe for Tuberculosis Detection. IEEE Sens J 22(15):14903–14910. https://doi.org/10.1109/JSEN.2022.3186995